Thickness control in electrogenerated mesoporous silica films by wet etching and electrochemical monitoring of the process

Taisiia Sikolenko, Christelle Despas, Neus Vilà, Alain Walcarius

Electrochemistry Communications 100 (2019) 11–15

Contents lists available at ScienceDirect

Electrochemistry Communications

journal homepage: www.elsevier.com/locate/elecom

Short communication

Thickness control in electrogenerated mesoporous silica films by wet etching and electrochemical monitoring of the process

Taisiia Sikolenko, Christelle Despas, Neus Vilà, Alain Walcarius*

Laboratoire de Chimie Physique et Microbiologie pour les Matériaux et l'Environnement (LCPME), UMR 7564, CNRS-Université de Lorraine, Villers-lès-Nancy 54600, France

ARTICLE INFO

Keywords:
Oriented mesoporous silica membrane
Ferrocene functionalized thin film
Wet etching
Film thickness control
Electroactive organic-inorganic hybrid

ABSTRACT

Vertically aligned mesoporous silica films can be generated by electrochemically assisted self-assembly (EASA) but the accurate control of their thickness is essentially restricted to the 100 nm range. Here we have developed a wet etching approach using dilute ammonium fluoride to gradually decrease the thickness of ferrocene-functionalized films down to 20 nm by increasing the etching time. The effectiveness of the process was followed by monitoring the decrease in the voltammetric response of ferrocene moieties that are progressively removed from the electrode surface upon silica etching. Film thickness variations have also been confirmed by profilometry and were consistent with the electrochemical measurements. Electron microscopy analyses indicated a uniform thickness decrease but also some loss in the integrity of the mesostructure after prolonged etching.

1. Introduction

Nanostructured electrode surfaces have gained importance in recent years for applications in various fields (e.g., energy conversion and storage [1,2], electronics and optoelectronics [3,4], sensors and biosensors [5,6]). Electrodeposition methods have played a special role in producing a wide range of nanostructured materials [7–9], which sometimes exhibit improved characteristics in comparison to materials produced by conventional techniques [10]. In particular, silica-based nanomaterials have attracted considerable interest from the electrochemistry community because these materials can be prepared in a variety of functionalized forms with tailored and organized structures at the nanoscale [11–13]. In this context, ordered mesoporous silica thin films have been generated on electrodes using chemical or electrochemical synthetic methods [14,15] and their performance was dramatically dependent on all features likely to affect mass transfer processes [14–18], the most critical point being the necessity to produce coatings with pores accessible from the film surface [19].

The best way to achieve this goal is by precise control of pore orientation, and an ideal configuration is given by films with uniaxially oriented one-dimensional mesochannels, with promising applications notably for electroanalytical purposes [13,20]. The most versatile methods available to date to produce small-pore (∅ 2–3 nm) vertically aligned mesoporous silica films on electrodes are: (i) Stöber-solution growth [21] and (ii) electrochemically assisted self-assembly (EASA) [22]. Oriented films with organo-functional groups covalently bonded to the silica walls can be also generated by EASA [23]. Although the thickness of electrogenerated mesoporous silica deposits can be tuned to some extent in the range of typically 100 nm by adjusting the synthesis parameters (i.e., deposition time and silica precursor concentration), scaling-up has been restricted by the formation of silica aggregates when attempting to get thick films (due to bulk precipitation in the diffusion layer), while scaling-down to ultra-thin films was not possible due to the absence of self-assembly at very short deposition times, t_{dep}, or very low precursor concentration (no film growth at $t_{dep} < 10$ s and silane concentration < 75 mM [24]). For instance, one can generate non-ordered ultrathin silica films by electrodeposition from very dilute precursor solutions [25], but nanostructured deposits cannot be produced as the EASA method requires a surfactant content above the critical micellar concentration and a silane/surfactant molar ratio larger than 0.78 [24]. To circumvent the first limitation, we have recently proposed a multilayer electrogeneration approach which makes it possible to obtain films with thicknesses of up to 400 nm [26]. Here, we now propose a post-treatment strategy to decrease the thickness of mesoporous silica films prepared by EASA. Although some approaches for thickness control of nanostructured silica membranes have been previously reported, they are not applicable to either vertically-aligned or small-pore mesoporous silica thin films [27–31].

The objective of the present work is thus to evaluate how tuning the thickness of oriented mesoporous silica films generated by EASA can be

* Corresponding author.
E-mail address: alain.walcarius@univ-lorraine.fr (A. Walcarius).

https://doi.org/10.1016/j.elecom.2019.01.013
Received 21 December 2018; Received in revised form 14 January 2019; Accepted 15 January 2019
Available online 16 January 2019

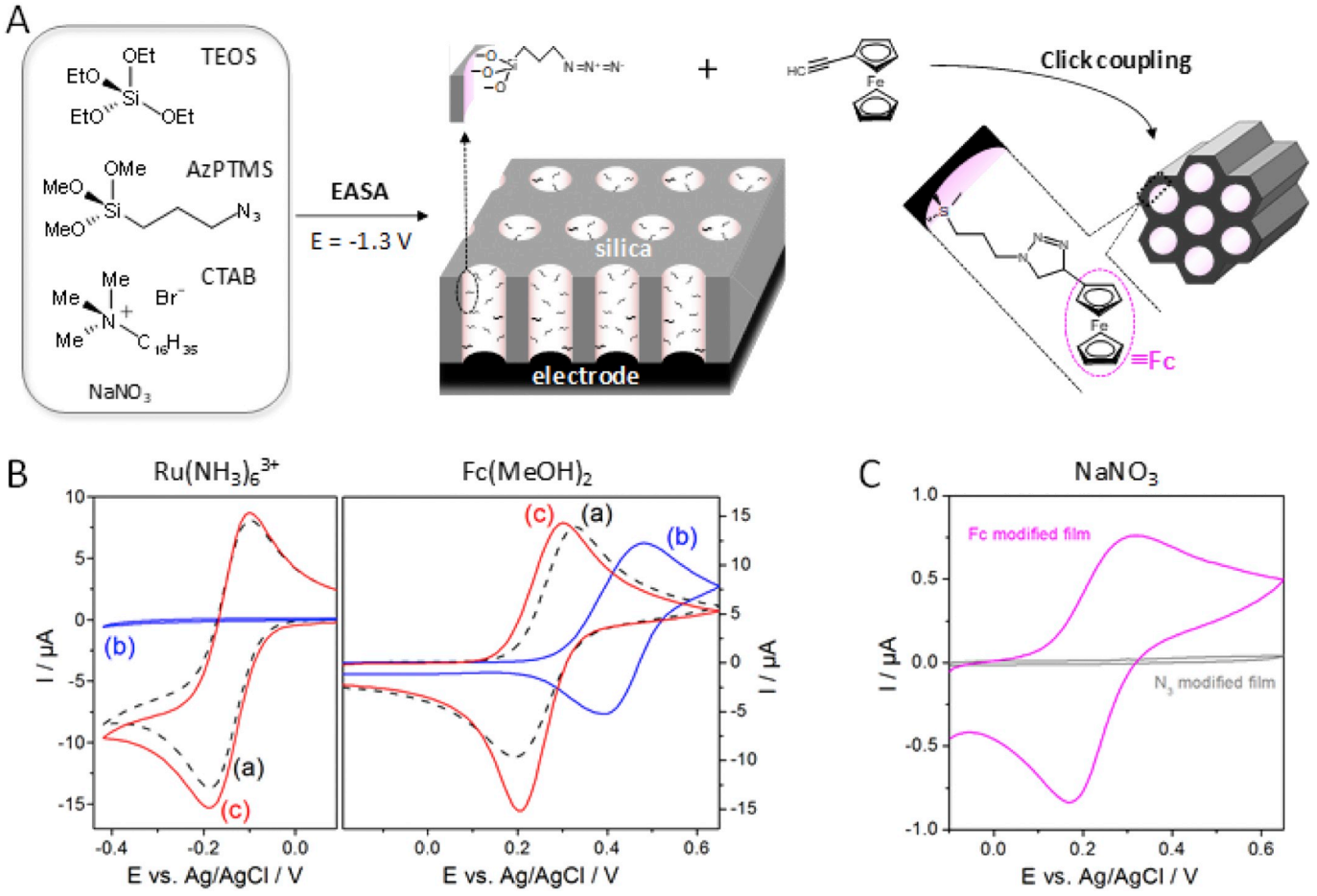

Fig. 1. (A) Scheme showing the preparation of ferrocene-functionalized films by EASA and click coupling; (B) CV curves recorded in 0.5 mM $Ru(NH_3)_6Cl_3$ (left) or 0.5 mM $Fc(MeOH)_2$ (right) using (a) a bare ITO or (b,c) an ITO covered with azide-functionalized mesoporous silica film (b) before or (c) after surfactant removal (supporting electrolyte: 0.1 M $NaNO_3$; potential scan rate: 50 mV s^{-1}); (C) CV curves recorded in 0.1 M $NaNO_3$ using ITO electrodes covered with mesoporous silica film bearing azide (N_3) or ferrocene (Fc) groups.

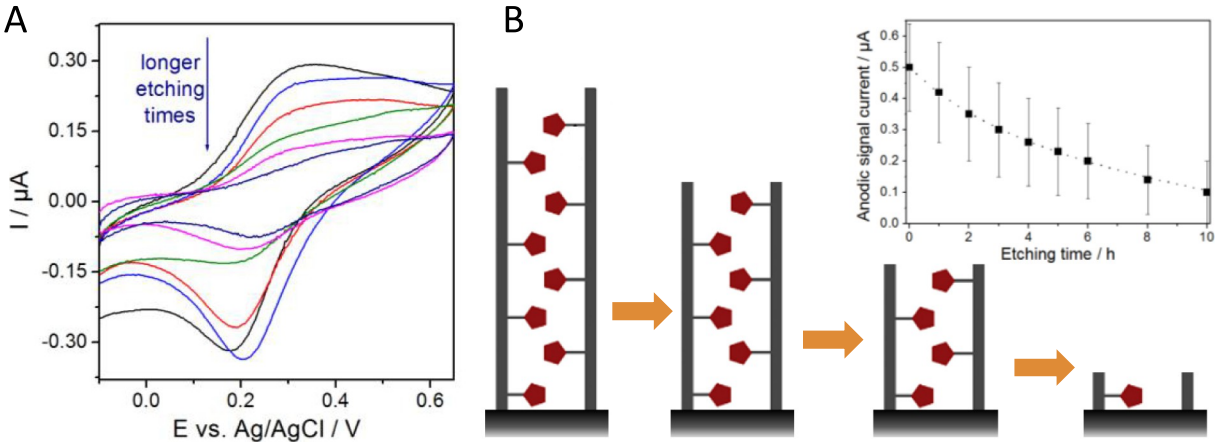

Fig. 2. (A) CV curves recorded in 0.1 M $NaNO_3$ (at 5 mV s^{-1}) using an ITO electrode covered with mesoporous silica film bearing ferrocene groups, which had been treated in 0.05 M NH_4F for 0, 1, 2, 4, 7 and 10 h. (B) Variation of the anodic signal with etching time (average of results obtained with six different films) and schematic illustration of the film thickness decrease upon etching (red pentagon = ferrocene). (For interpretation of the references to colour in this figure legend, the reader is referred to the web version of this article.)

realized by wet etching using dilute ammonium fluoride (NH_4F) solutions. Stronger etchants (such as HF or NaOH) must be avoided because they lead to complete dissolution of the silica or non-uniform attack leading to rough layers [32,33], whereas NH_4F appears to be soft enough for the purpose of slow film etching (as recently shown for hydrophobic and large-pore 3-dimensional mesoporous materials [34]). The results of film etching have been monitored by profilometry, electrochemical methods (cyclic voltammetry) and electron microscopy analyses, using ferrocene-functionalized mesoporous materials. This can be more informative than operating with non-functionalized silica

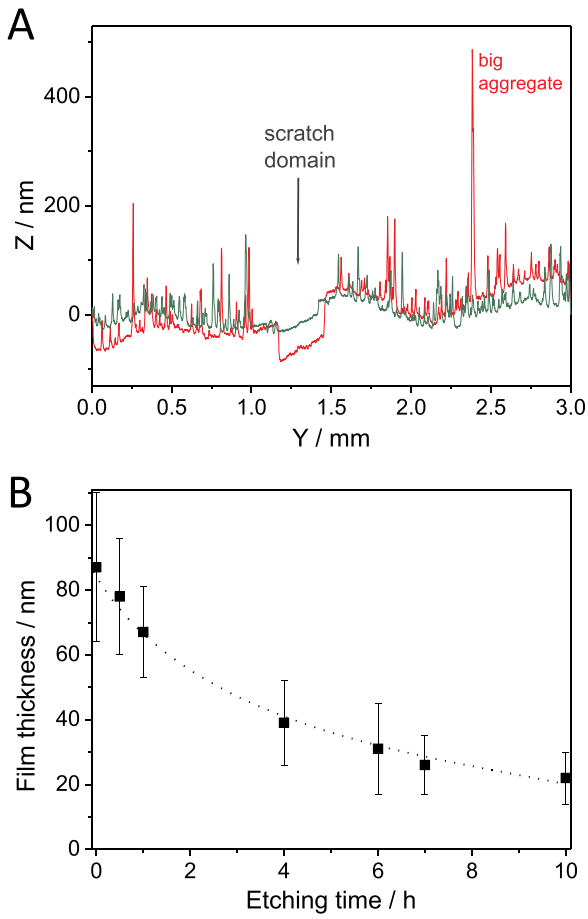

Fig. 3. (A) Typical profilometry measurements (red, before etching, and green, after etching); (B) Variation of film thickness upon etching over increasing periods of time (eight different films, six distinct profilometry measurements per film). (For interpretation of the references to colour in this figure legend, the reader is referred to the web version of this article.)

films, as the voltammetric response of the ferrocene groups can be used to monitor the etching process.

2. Experimental section

2.1. Preparation of ferrocene-functionalized and oriented mesoporous silica films on ITO electrode

Azide-functionalized silica films were first generated on indium-tin oxide (ITO) plates (surface resistivity 8–12 Ω, Delta Technologies) by EASA [23]. The sol was made of an ethanol:water solution (1:1) containing 80 mM TEOS (tetraethoxysilane, 98%, Alfa Aesar), 20 mM AzPTES (azidopropyltriethoxysilane, prepared as in [23]), 32 mM CTAB (cetyltrimethylammonium bromide, 99%, Acros Organics) and 0.1 M $NaNO_3$, which was set to pH 3 using 1 M HCl (Prolabo), and aged for 2 h at room temperature. Film deposition was performed potentiostatically at a negative potential of −1.3 V for 20 s, using a three-electrode system (ITO working electrode, silver rod as pseudo-reference electrode and stainless steel plate as counter electrode) and a μAutolab III potentiostat operated by GPES software. The resulting films were rinsed with distilled water and kept overnight at 130 °C. After template extraction (in 0.1 M HCl ethanol solution for 15 min), the covalent bonding of the ferrocene species was achieved by a 'click reaction' between azide-containing films and ethynylferrocene. This was carried out in DMF/H_2O media (12 ml dimethylformamide (DMF, 99.94%) + 8 ml water) containing 10 mg ethynylferrocene (97%, Aldrich), 3 mg copper acetate dihydrate (UCB) and 7.5 mg ascorbic acid (99.7%, Merck). The reaction was conducted at room temperature for 20 h in the absence of light. The films were cleaned to remove traces of the catalyst using an ethanol solution of 0.05 M diethyldithiocarbamate trihydrate (DDTC, Sigma Aldrich) for 30 min, and then rinsed with ethanol.

2.2. Etching procedure and film characterization

Ferrocene-functionalized mesoporous silica films were etched with a 200 μl drop of 0.05 M ammonium fluoride (NH_4F, 98%, Prolabo) under cover for the chosen time (in the 0–10 h range, under quiescent conditions). After etching, the samples were washed thoroughly with deionized water and air-dried. Their thickness was estimated from profilometry measurements, performed before and after etching, using the Dektak XT apparatus with Vision 64 software (Brüker). Their electrochemical response was characterized by cyclic voltammentry (CV) in 0.1 M $NaNO_3$ using an EM Stat2 potentiostat (PalmSens). Some samples were imaged by electron microscopy (surface analysis by SEM using the JEOL JCM-6000 microscope and mesostructure observation by TEM with Philips CM20 microscope at an acceleration voltage of 200 kV).

3. Results and discussion

Fig. 1A illustrates schematically the film preparation process, which involves the electrochemically assisted self-assembly (EASA) of an ordered, azide-functionalized and vertically aligned mesoporous silica membrane and its subsequent click coupling with ethynylferrocene [23]. EASA is a known electrodeposition method based on the application of a cathodic potential to an electrode immersed in a hydrolyzed sol solution containing silica precursors (TEOS and AzPTES in this case), which condense due to the electrochemically induced local pH increase on the cathode, with a cationic surfactant (CTAB) acting as a structure-directing agent, ensuring the growth of hexagonally-packed mesochannels orthogonal to the underlying electrode surface [22–24]. The supporting electrolyte, $NaNO_3$, also contributes to the cathodic generation of OH^- ions [35–37]. Fig. 1B shows that the azide-functionalized film was uniformly deposited over the whole electrode surface area and was crack-free (no voltammetric signal recorded for the Ru$(NH_3)_6^{3+}$ redox probe prior to surfactant removal, while ferrocene dimethanol ($Fc(MeOH)_2$) is likely to be detected only due to the possible solubilization of such neutral species in the surfactant phase; see blue curves in Fig. 1B). After template removal, the film was highly porous (see the large voltammetric signals observed for both Ru$(NH_3)_6^{3+}$ and $Fc(MeOH)_2$ probes in Fig. 1B, red curves), confirming the good accessibility of azide groups for further functionalization with ferrocene moieties. The effectiveness of click coupling is demonstrated by the well-defined voltammetric signal obtained for the ferrocene grafted film (thanks to electron hopping between adjacent redox centers in the mesopore channels) whereas no noticeable response was observed with the azide functionalized membrane (Fig. 1C). When operating at a low potential scan rate ($< 10\ mV\ s^{-1}$), all ferrocene groups are electrochemically accessible (the voltammetric peak currents are characteristics of thin-layer behavior [38]), thus providing a good method for quantitative monitoring of film thickness variations upon etching.

This is illustrated in Fig. 2A, which shows a progressive decrease in peak currents on increasing the duration of film treatment in NH_4F prior to voltammetric analysis in the electrolyte solution. This suggests a continuous film etching, at a rather slow rate, as the progressive dissolution of the silica network would result in leaching more and more ferrocene into the solution and thus there would be less ferrocene in the film available for voltammetric detection (Fig. 2B). In order to confirm effective film etching (and not just ferrocene loss from the material), additional film thickness measurements (Fig. 3) have been performed by profilometry on scratched samples to evaluate thickness

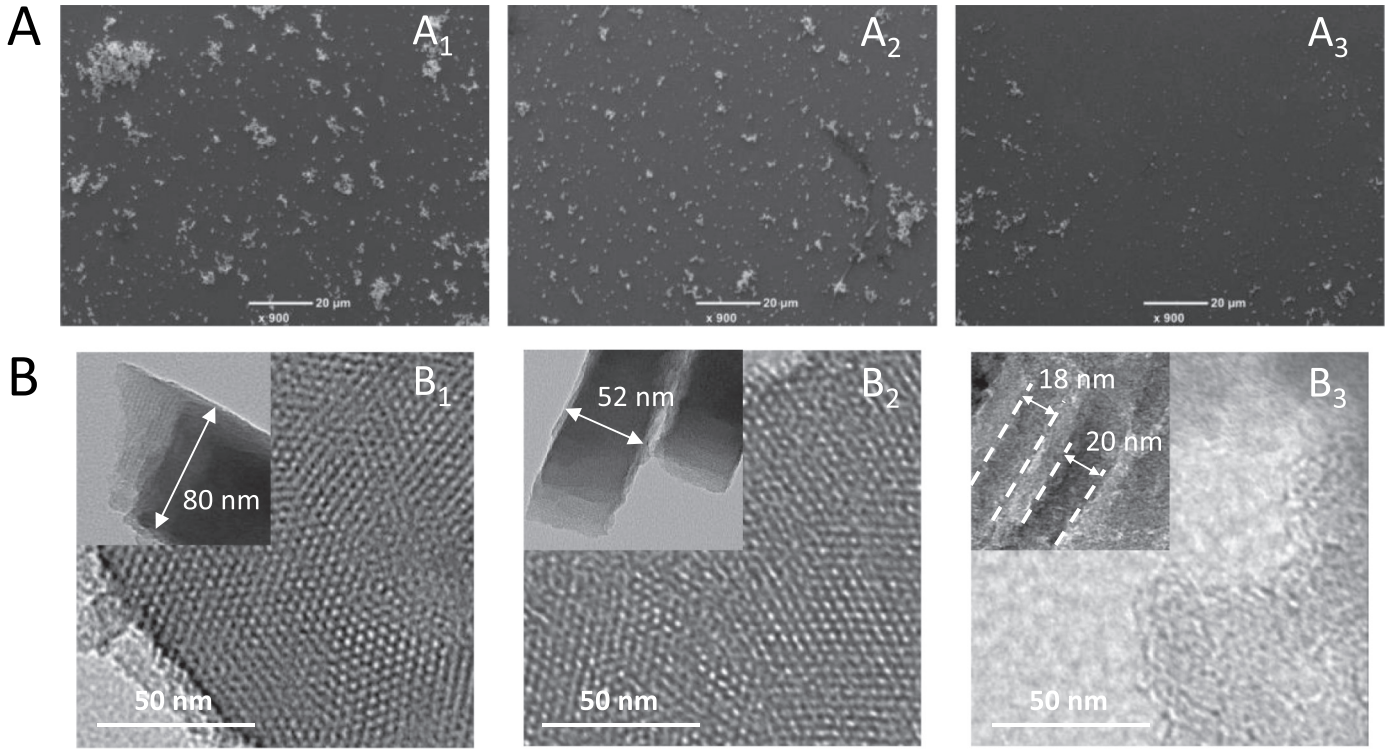

Fig. 4. (A) SEM and (B) TEM imaging (1) before and (2,3) after moderate and long etching times, corresponding to film thicknesses of about 50 and 20 nm, respectively.

variations upon reaction with NH_4F. In spite of rather noisy responses (Fig. 3A), originating mainly from the presence of silica particles/aggregates on top of the films (as is common for EASA-based deposits [22,24]), a clear trend can be drawn on the basis of multiple profilometry measurements made on various films etched for different periods of time (Fig. 3B). As shown, prolonged treatments in NH_4F resulted in a progressive decrease in film thickness, confirming the suitability of NH_4F for controlled wet etching of the silica material [34], in contrast to stronger reagents such as HF (which leads to complete dissolution of the silica film within seconds) or NaOH (which is known to rapidly destroy the structure of mesoporous silica [39]). The evolution of both electrochemical (Fig. 2B) and profilometry (Fig. 3B) data being similar, one can conclude that cyclic voltammetry is a satisfactory technique for monitoring the effectiveness of wet etching applied to a mesoporous silica film bearing redox-active moieties such as ferrocene. The quite large error bars do not mean that the thickness is hard to control; these are due to the fact that the etching experiments were carried out using numerous different starting films which already exhibited quite a large distribution in thickness and ferrocene content.

Effective etching was also demonstrated using electron microscopy (Fig. 4). Imaging by SEM reveals not only that the mesostructured thin film is dissolved by NH_4F but also that the overlaying aggregates/particles tend to disappear upon prolonged etching (Fig. 4A), consistent with the roughness decrease observed by profilometry (Fig. 3A). TEM views confirm that the regular mesostructure and pore orientation are maintained upon moderate wet etching and that the process is uniform over the whole film surface area (uniform film thickness), but also that prolonged etching leads to some damage in the mesostructure (becoming wormlike instead of hexagonal) (Fig. 4B). Note that in spite of the loss in quality of the mesostructure, the ferrocene groups in the material remained electrochemically accessible, yet led to less well-defined CV responses (Fig. 2A). The progressive shape changes in the CV curves and shift in peak currents towards more anodic values are in agreement with restricted transport phenomena reported previously for such oriented mesoporous silica films bearing redox moieties [38].

4. Conclusion

In this work, we have demonstrated the possible wet etching of electrogenerated, vertically-aligned and ferrocene-functionalized, mesoporous silica thin films by treatment in NH_4F. The process has been characterized by profilometry measurements and electrochemical monitoring, both of which confirm the progressive decrease in film thickness upon increasing the contact time with etchant solution. The integrity of the regular mesostructure and pore orientation were maintained, except for very long etching times when some loss of order was observed while keeping the redox probes attached to the silica framework electrochemically accessible.

Acknowledgements

The authors gratefully thank Liang Liu (LCPME, Nancy) for advice in profilometry measurements and Jaafar Ghanbaja (IJL, Nancy) for TEM analysis. T.S. acknowledges a PhD grant from the University of Lorraine.

References

[1] M. Noked, C. Liu, J. Hu, K. Gregorczyk, G.W. Rubloff, S.B. Lee, Acc. Chem. Res. 49 (2016) 2336–2346.
[2] E. Tsuji, Electrochemistry 84 (2016) 667–673.
[3] W. Wu, Nanoscale 9 (2017) 7342–7372.
[4] M. Morales-Masis, S. De Wolf, R. Woods-Robinson, J.W. Ager, C. Ballif, Adv. Electron. Mater. 3 (2017) 1600529.
[5] A. Walcarius, A. Kuhn, Trends Anal. Chem. 27 (2008) 593–603.
[6] I. Taurino, G. Sanzo, R. Antiochia, C. Tortolini, F. Mazzei, G. Favero, G. De Micheli, S. Carrara, Trends Anal. Chem. 79 (2016) 151–159.
[7] F. Nasirpouri, Electrodeposition of Nanostructured Materials, Springer Series in Surface Sciences vol. 62, (2016).
[8] A. Lahiri, F. Endres, J. Electrochem. Soc. 164 (2017) D597–D612.
[9] C. Li, M. Iqbal, J. Lin, X. Luo, B. Jiang, V. Malgras, K.C.-W. Wu, J. Kim, Y. Yamauchi, Acc. Chem. Res. 51 (2018) 1764–1773.
[10] I. Gurrappa, L. Binder, Sci. Technol. Adv. Mater. 9 (2008) 043001.
[11] A. Walcarius, Chem. Soc. Rev. 42 (2013) 4098–4140.
[12] A. Walcarius, Electroanalysis 27 (2015) 1303–1340.

[13] A. Walcarius, Curr. Opin. Electrochem. 10 (2018) 88–97.
[14] M. Etienne, A. Quach, D. Grosso, L. Nicole, C. Sanchez, A. Walcarius, Chem. Mater. 19 (2007) 844–856.
[15] M. Etienne, Y. Guillemin, D. Grosso, A. Walcarius, Anal. Bioanal. Chem. 405 (2013) 1497–1512.
[16] O. Sel, S. Sallard, T. Brezesinski, J. Rathousky, D.R. Dunphy, A. Collord, B.M. Smarsly, Adv. Funct. Mater. 17 (2007) 3241–3250.
[17] D. Fattakhova-Rohlfing, M. Wark, J. Rathousky, Chem. Mater. 19 (2007) 1640–1647.
[18] M. Etienne, J. Cortot, A. Walcarius, Electroanalysis 19 (2007) 129–138.
[19] U.-H. Lee, M.-H. Kim, Y.-U. Kwon, Bull. Kor. Chem. Soc. 27 (2006) 808–816.
[20] F. Yan, X. Lin, B. Su, Analyst 141 (2016) 3482–3495.
[21] Z. Teng, G. Zheng, Y. Dou, W. Li, C.Y. Mou, X. Zhang, A.M. Asiri, D. Zhao, Angew. Chem. Int. Ed. 51 (2012) 2173–2177.
[22] A. Walcarius, E. Sibottier, M. Etienne, J. Ghanbaja, Nat. Mater. 6 (2007) 602–608.
[23] N. Vilà, J. Ghanbaja, E. Aubert, A. Walcarius, Angew. Chem. Int. Ed. 53 (2014) 2945–2950.
[24] A. Goux, M. Etienne, E. Aubert, C. Lecomte, J. Ghanbaja, A. Walcarius, Chem. Mater. 21 (2009) 731–741.
[25] F. Qu, R. Nasraoui, M. Etienne, Y. Bon Saint, A. Côme, J. Kuhn, J. Lenz, R. Gajdzik, A. Walcarius Hempelmann, Electrochem. Commun. 13 (2011) 138–142.
[26] G. Giordano, N. Vilà, E. Aubert, J. Ghanbaja, A. Walcarius, Electrochim. Acta 237 (2017) 227–236.
[27] L.C. Huang, E.K. Richman, B.L. Kirsch, S.H. Tolbert, Microporous Mesoporous Mater. 96 (2006) 341–349.
[28] J. Hwang, N. Shoji, A. Endo, H. Daiguji, Langmuir 30 (2014) 15550–15559.
[29] K.-C. Kao, C.-H. Lin, T.-Y. Chen, Y.-H. Liu, C.-Y. Mou, J. Am. Chem. Soc. 137 (2015) 3779–3782.
[30] K. Wan, Z.-P. Yu, Q.-B. Liu, J.-H. Piao, Y.-Y. Zheng, Z.-X. Liang, RSC Adv. 6 (2016) 75058–75062.
[31] X. Ma, X. Su, J. Zhang, M. Dang, J. Tao, P. Xu, Y. Li, P. Lv, W. Wei, J. Porous. Mater. 25 (2018) 489–494.
[32] L.F. Dumée, F. She, M. Duke, S. Gray, P. Hodgson, L. Kong, Nano 4 (2014) 686–699.
[33] Y. Minhao, M.J. Henderson, A. Gibaud, Thin Solid Films 517 (2009) 3028–3035.
[34] M. Kobayashi, K. Susuki, T. Otani, S. Enomoto, H. Otsuji, Y. Kuroda, H. Wada, A. Shimojima, T. Homma, K. Kuroda, Nanoscale 9 (2017) 8321–8329.
[35] I. Katsounaros, G. Kyriacou, Electrochim. Acta 53 (2008) 5477–5484.
[36] R. Shacham, D. Avnir, D. Mandler, Adv. Mater. 11 (1999) 384–388.
[37] P.H. Ho, E. Scavetta, F. Ospitali, D. Tonelli, G. Fornasari, A. Vaccari, P. Benito, Appl. Clay Sci. 151 (2018) 109–117.
[38] N. Vilà, A. Walcarius, Electrochim. Acta 179 (2015) 304–314.
[39] S. Sayen, A. Walcarius, J. Electroanal. Chem. 581 (2005) 70–78.